Heliyon 9 (2023) e22870

Contents lists available at ScienceDirect

Heliyon

journal homepage: www.cell.com/heliyon

# Developing an efficient climate forecasting model for the spatiotemporal climate dynamics estimation and the prediction that fits the variable topography feature of the upper Blue Nile basin, Ethiopia

Megbar Wondie [a,*], Titike Kassa [b], Demeke Fisseha [c]

[a] Atmospheric Physics and Radar Meteorology Research Division at Debre Markos University, Ethiopia
[b] Atmospheric and Climate Science Unit, Ethiopian Space Science and Technology Institute (ESSTI), Ethiopia
[c] Department of Mathematics, Debre Markos University, Ethiopia

ARTICLE INFO

*Keywords:*
Precipitation
Temperature
Climate
Model
Prediction

ABSTRACT

The spatiotemporal climate estimation and prediction are challenging and demanding for variable topography feature areas. Spatially, the upper Blue Nile basin (UBNB) is unsatisfactory owing to complex topographical features and the lack of accurate climate prediction and estimation models. Yet accurate information and reliable seasonal climate dynamics estimation and forecasting are essential in the region for controlling reservoir operation and flooding prevention. However, there is a lack of reports regarding the accuracy and predictability of the climate in the UBNB region. Therefore, this article aims to improve the Artificial Neural Network (ANN) model by adopting the Impulse Response Function (IRF) and comparing it to the Regional Climate Model (RCM) and European Centre of Medium-range Weather Forecast (ECMWF) models for spatiotemporal climate dynamics estimation and forecasting, which are reliant on the UBNB topography features. Different atmospheric parameter data are investigated from reanalysis models. A fast Fourier transform is applied to remove the redundancy of the data and avoid the computational cost. The RCM and ECMWF models are used to test the performance of ANN model prediction skills. The IRF model was applied to enhance the ANN model's climate prediction performance. A 12-month spatial variation of precipitation is analyzed. The ANN model showed a satisfactory prediction performance, better than the RCM and ECMWF models by 20 %. After increasing the ANN model performance by IRF, the prediction errors are reduced by 10.2 % for precipitation and by 7.9 % for temperature. Based on the model results, the temperature has increased over the past 40 years and is expected to continue for the coming three decades (30 years). In contrast, precipitation over the past 40 years has decreased, and a slight increment will be expected in the next eight years, from 2024 to 2029. Therefore, this model should be practiced across Ethiopia and the Globe for accurate prediction of climate patterns. Hence, clear awareness should be created for the local community by providing a scientific remedy for future climate conditions to reduce production risk.

* Corresponding author.
*E-mail address:* megbar.radiation05@gmail.com (M. Wondie).

https://doi.org/10.1016/j.heliyon.2023.e22870
Received 25 April 2023; Received in revised form 21 November 2023; Accepted 21 November 2023
Available online 27 November 2023

## 1. Introduction

In Ethiopia's upper Blue Nile Basin (UBNB), more than 85 % of the population lives in subsistence farming [1,2]. However, crop production is reliance on rain-fed agriculture [2,3]. Hence, with various triggers of climate change, crop production is below a satisfactory level [4–7]. Climate change acts as the source of reasons for the occurrence of extreme events which reduced crop production around the globe, particularly in developing countries such as UBNB in Ethiopia [1]. This is because UBNB's geography is so diverse that it is vulnerable to climate change (droughts and floods occur frequently). In line with climate change and variability, at the current time (2023), UBNB society is stressed by food insecurity problems and is exposed to extreme hunger [7,8]. Therefore, accurate climate estimation and prediction for early warning systems are a matter of survival [5,9]. Hence, the future plan of the national policies and strategies prioritizes supporting the agriculture sector by providing accurate climate change estimation and prediction for food security [7]. Hence, such information can support making the right decision regarding crop selection, which can adapt to future climate conditions and reduce crop production risk [10]. However, due to variable topographic features, accurate climate (precipitation and temperature) prediction over UBNB is not convincing [6].

To overcome those challenges, different scholars, e.g., Getachew and Yuei [11], tried to model climate prediction using the ANN model, and they got good results for the UBNB. Despite not being cogent for a long-year climate prediction, this is because of the limited evidence to understand the Atmosphere-Biosphere-Hydrosphere interactions and the lack of modern measurement techniques at UBNB to parameterize the model and its processes [11]. Therefore, a deep understanding of the nature of atmospheric dynamics is quite useful in applying powerful computational skills to the dynamic and physical model parameters to tackle accurate climate prediction failure [12].

Several studies examined the predictability of precipitation in the UBNB by applying statistical approaches such as Bayesian and classical models [13,14]. However, due to the nonlinear nature of precipitation and temperature, statistical technique prediction is below a satisfactory level (the correlation coefficient between the observed and predicted parameters is less than 0.5) [14,15]. Furthermore, dynamic models (RCM and ECMWF) have been used for climate predictions in different parts of the world [16–20]. However, ECMWF and GCM can predict the climate parameters only at grid points, which require downscaling to the regional level, which leads to significant (27 %) uncertainties [21,22]. Furthermore, the effectiveness of statistical models has not been adequately evaluated so far. The previous studies have either used dynamic (ECMWF and RCM) models to compare different emission scenarios or stationery (statistical) models without considering the impact of Global warming [19,23].

Therefore, different scholars tried to develop a simulation model such as the ANN for variable topography feature areas in climate prediction. For instance, Singh and Borah [24], Funk et al. [25], Neelam et al. [26] in India, Mislan et al. [27] in Indonesia, Rajendra et al. [28] in Ongole, and Katherine et al. [29] over the Globe. Hence, the ANN model has reduced the high-priced RCM and ECMWF

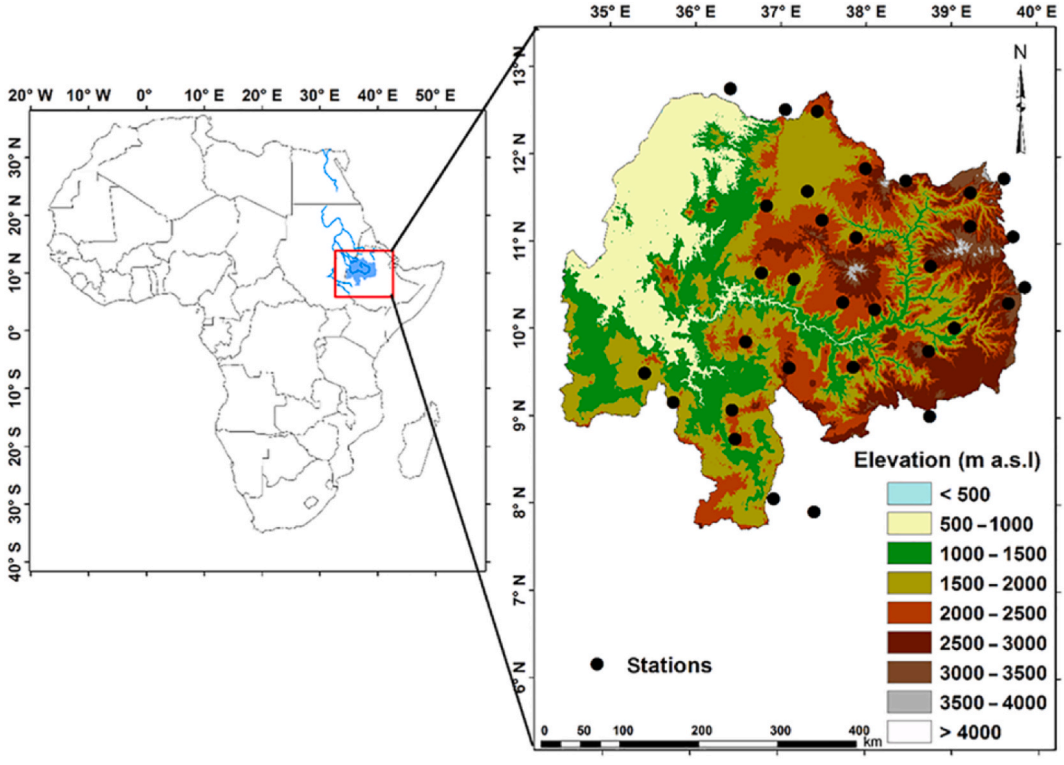


**Fig. 1.** Location map of UBNB, Ethiopia [34].

models for climate research [1,30–32]. Furthermore, the ANN model considers the nonlinearity, flexibility, and data-driven nature of atmospheric parameters to build models [33]. However, the ANN model's potential is not effective for long-term (more than 20 years) climate prediction. As far as our reading is concerned, there is no previous study to predict precipitation and temperature by improving the ANN model through IRF for long-term prediction over UBNB. Therefore, this paper is aimed at improving the ANN model by IRF for the UBNB spatiotemporal climate prediction by checking its performance with the RCM and ECMWF models.

## 2. Study area description, data, and methodology

### 2.1. Study area description

The UBNB is located in the tropical region and the range of the degree location is found between 7.40° to 12.50° latitudes and from 34.25° to 39.49° longitudes, with a drainage area of 176,000 $km^2$. Besides this, the range of elevation varied from 500 to 4160 m and the main economic activity is rain-feed agriculture [34]. Hence, the mean annual precipitation and the mean daily temperature varied from 1040 to 1600 mm and 18–23 $C^0$, respectively [35]. Specifically, its hydrological behavior is characterized by high spatiotemporal variability due to its variable topographic features which vary from cold to hot within a limited elevation range [34–37]. The elevation range and the station distribution of the study area are provided in Fig. 1.

### 2.2. Data sources

UBNB is one of the data-scarce regions due to less density and irregular orientations of ground-based measurements [34]. To resolve this challenge, gridded precipitation, temperature, evaporation, surface pressure, downward radiation, zonal wind (U), and meridional wind (V) at 10 m altitude history and prediction data is obtained from the ECMWF products from 1981 to 2020. The spatial resolution of ECMWF data is 0.125° by 0.125° and it has a daily temporal resolution [35]. The data is available on the website https://cds.climate.copernicus.eu. Furthermore, for comparison purposes of the prediction skills of the model, precipitation and temperature history and prediction data are obtained from RCM. The spatial resolution of RCM is 0.11° by 0.11° and the temporal resolution is daily. The data are available on the website http://www.data.African-cordex.net. According to the study conducted by Ref. [35], ECMWF model data is well agreed with the ground-based data. The reliable information on the data sources and the study period is provided in Table 1. The data was analyzed using MATLAB software and Climate Data Operator (CDO).

### 2.3. Methodology

The resolution of RCM and ECMWF data is not the same for comparison purposes and is not too enough to estimate the required climate parameters on a small scale. Besides this, to interpolate RCM 0.1 by 0.1° and ECMWF 0.125 by 0.125° to 0.05 by 0.05-degree resolution using climate data operator (CDO) software through wavelet transform model in the Linux environment. The performance of RCM and ECMWF are checked by Megbar [38] based on 34 areal weighted average interpolation ground observations using error matrices. Interested readers can refer to the mentioned reference. The schematic diagram (Fig. 2 (a)) and the ANN model hidden layers (Fig. 2 (b)) are designed to increase the clarity of the model improvement procedures and the model structure. Fast Fourier Transform is applied to remove the redundancy of the data to avoid computational costs.

#### 2.3.1. The input variables of the model

The 40 years of daily data (1981–2020) has 14,610 samples at a grid point and it is arranged rows-wise which are imported into the MATLAB workspace. According to the findings, Kumar et al. [12] used 60 % of the samples for training, 20 % samples for the validation network, and the remaining 20 % samples for the test. The study conducted by Ref. [39] confirmed that 70 % of the samples were fed to the training network, 20 % for validation, and 10 % for the test that satisfied their model requirements. This paper tests the two researchers' procedures based on MATLAB algorism. However, to design 70 % for training, 15 % for validation, and 15 % for the test which satisfied the ANN model requirement after improvement by IRF that fits the UBNB climate.

#### 2.3.2. The model improvement

A function of climate elements (precipitation, temperature) = coefficient (precipitation) + coefficient (temperature). However, the climate is a complex system that varies with time and space depending on the precipitation, temperature, and current wind vector changes. The model structure is an important step in building an optimal ANN model for UBNB. The effect of the system on the input data can be described by a mathematical function. Hence, the relationship between the input data ($x_j$) of a system and its output values (g) was described by the convolution integral equation [39,40].

**Table 1**
Different climate data sources, spatiotemporal resolution per UBNB, time coverage, and website.

| Data types | data used | Time resolution | Space resolution | Website |
|---|---|---|---|---|
| RCM | 1981–2020 | daily | 0.11 by 0.11° | http://www.data.African-cordex.net |
| ECMWF | 1981–2020 | daily | 0.125 by 0.125° | https://cds.climate.copernicus.eu |

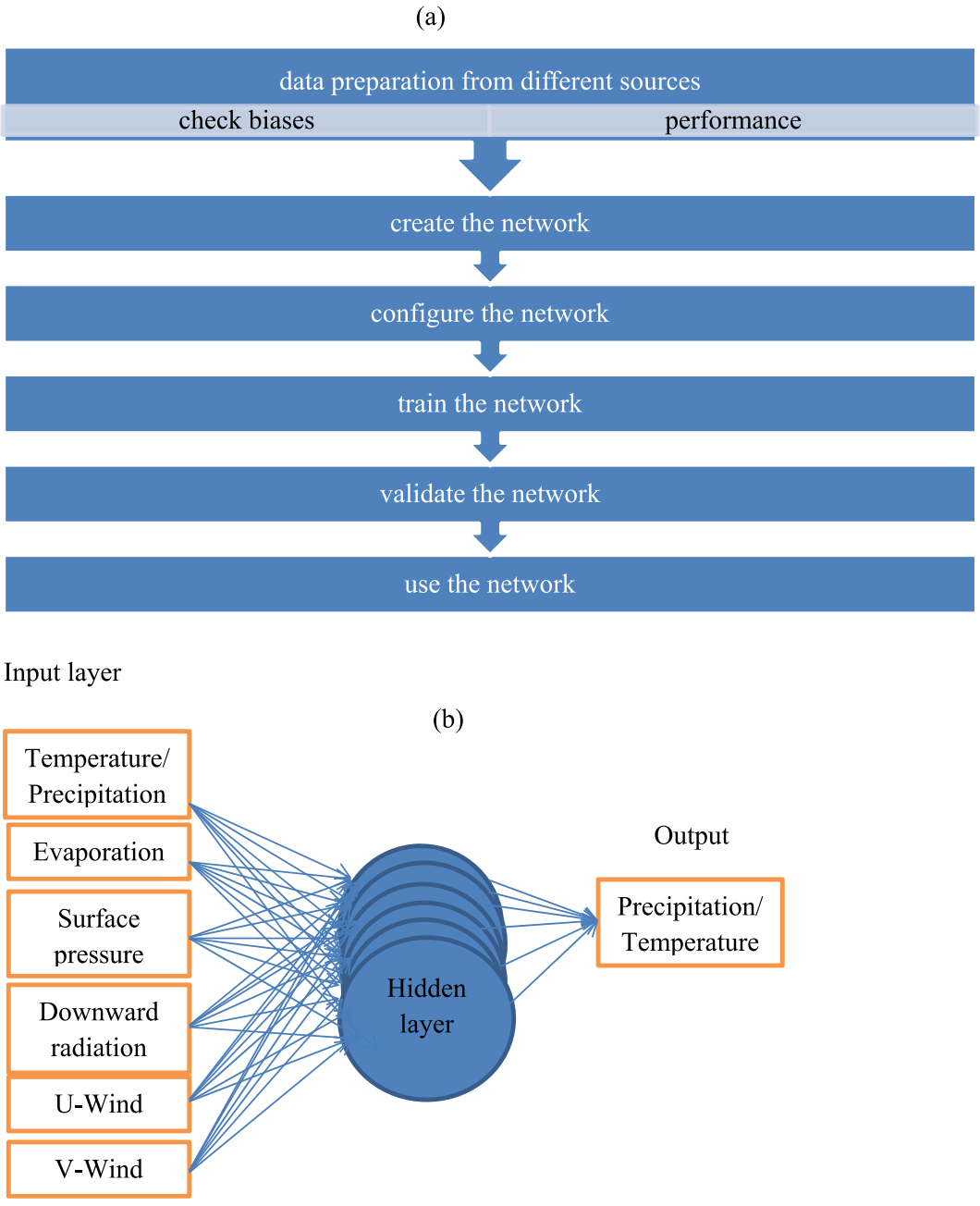


**Fig. 2.** A schematic diagram of the model structure (a) and architecture of multilayer ANN network (b) is organized for the prediction of temperature and precipitation.

$$g(t) = \int h(t-\tau) x_j(t) d\tau + \varepsilon(t) \tag{1}$$

where, $h(t-\tau)$, $x_j(t)$, g(t), and $\varepsilon(t)$ are impulse responses of a function, input data, output, and error due to measurement respectively. Therefore, (Eq. (1)) is IRF that is used to improve the existing ANN model. The ANN model has three layers, an input layer, a hidden layer, and an output layer as shown in Fig. 2 (b). The seven input layers (precipitation, temperature, U, V, downward solar radiation, evaporation, and surface pressure) are used to as the input attributes of the ANN model (see Fig. 2 (b)). The hidden layer is computationally determined by trial and error with an activation function of 0.01 [41]. The number of hidden nodes is iterated from 0 to 1000 epoch, and a decision is decided when the minimum error metrics (R, RMSE, BR, and MRE) are found. The development of the ANN model considering the bias denoted by $b_k$ and weighted function $w_{kj}$. The net input at the summing junction is written as

$$v_k = \sum_{j=1}^{m} w_{kj} x_j \tag{2}$$

where $x_j$ is the input data, which is controlled to the amplitude of the neuron to some finite value. The output of the kth neuron was semis-like (Eq. (3)) [14].

$$X_k = \varphi(v_k + b_k) \tag{3}$$

By considering Mackay Glass time series methods, IRF from (Eq. (1)) is feeding to the model in the form of 'b' and 'c' parameters as shown in (Eq. (4)).

$$y_k = -bX_k(t) + \frac{cX_k(t-\tau)}{1 + X_k{}^{10}(t-\tau)} \tag{4}$$

where b is represented g from (Eq. (1)) at the data sample t = 0 which is the slope of the function, and c is represented g from (Eq. (1)) at the data sample t = 14,610 which is $y_k$ intercept calculated by applying the least square method after to calculate $X_k$ from (Eq. (3)) and $\tau$ is instant time [41]. From 40 years of precipitation data, a maximum annual average value of 1300 mm and the minimum annual average value of 950 mm. Hence the bandwidth of the data is the difference between 1300 mm and 950 mm which is 350 mm. Owing to this, we took N = 700 samples for the prediction start time by applying Nyquist's theorem. Nyquist said that without lost information to take sample data greater than or equal to two times the bandwidth of the data (bandwidth (350) *2 = 700). After getting N, Eq. (4) is expanding for prediction purposes an algorism is written as

$$y_k(N+1) = y_k(N) - b * y_k(N) + \frac{c * y_k(N - tau)}{(1 + y_k(N - tau)^{\wedge}10)} \tag{5}$$

Where tau is a constant number that is equal to 17 [41]. The training model is prepared by

$$y_t = con2seq(y_k(1 : Nu)) \tag{6}$$

where, Nu is a parameter of the training algorithm and measures the adapting/learning rate of the network, to choose N/2 but having a freedom +50 or −50 [40], hence in this case, N/2–50 is used to increase the number of training data for adaptation purposes to improve the prediction skills of the model. When the maximum Nu is reached, the learning rate has maximized and further pieces of training are leading only to a validation stop or mostly, a minimum gradient. Con2seq means in computer code concurrent vectors to be converted to sequential vectors and back again. The validation model is prepared by

$$y_v = con2seq(y_k(Nu+1 : end)) \tag{7}$$

The test model is prepared from validation data by applying (Eq. (6))

$$y_n = y_t(end - \max(inputDelay)+1 : end) \tag{8}$$

By combining $y_v$ and $y_n$ to develop the following model

$$[z_1, z_2, z_3] = preparets(net, \{\}, [y_n\ y_v]) \tag{9}$$

Then the prediction (P) model from the training, validation, and testing is estimated as

$$P = net(z_1, z_2, z_3) \tag{10}$$

The errors between true (history) data and prediction data are calculated by

$$E = y_v - P \tag{11}$$

The training model is considered to check the goodness of the training progress. The gradient value of the validation has checked the performance of the ANN model. The performance has become a very small value while the training attains a minimum of the performance and the other two parameters are used to terminate the training. These adjustable parameters are smaller than predefined set values which are found at 0.089 for gradient and 0.213 for number validation, and then the training is stopped.

**Table 2**
The correlations between atmospheric parameters (atmospheric pressure (Pr), U wind, V wind, evaporation (E), and surface downward radiation (DR) with precipitation (P) and temperature (T)) data were done from 1981 to 2020.

| Parameter | T/P | Pr | U | V | E | DR |
|---|---|---|---|---|---|---|
| P | 0.544 | 0.208 | 0.189 | 0.385 | 0.687 | 0.516 |
| T | 0.544 | 0.362 | 0.229 | 0.323 | 0.704 | 0.413 |

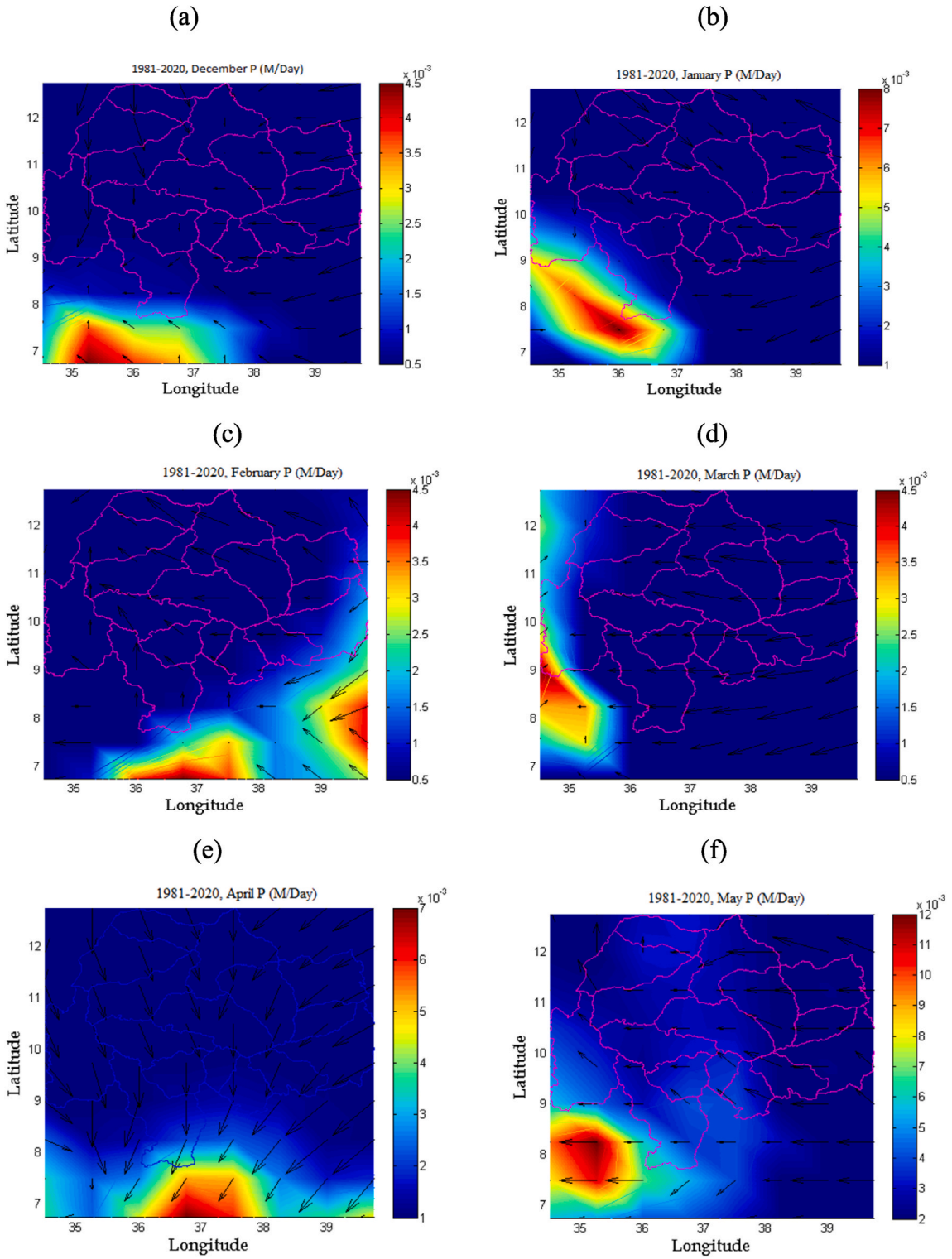


**Fig. 3.** Monthly variation of precipitation and wind direction from ECMWF model, the black arrow indicates wind direction. The description of precipitation and wind direction in each month indicated by Panel (a) for December, panel (b) for January, panel (c) for February, panel (d) for March, panel (e) for April, panel (f) for May, panel (g) for June, panel (h) for July, panel (i) for August, panel (j) for September, panel (k) for October, and panel (l) for November.

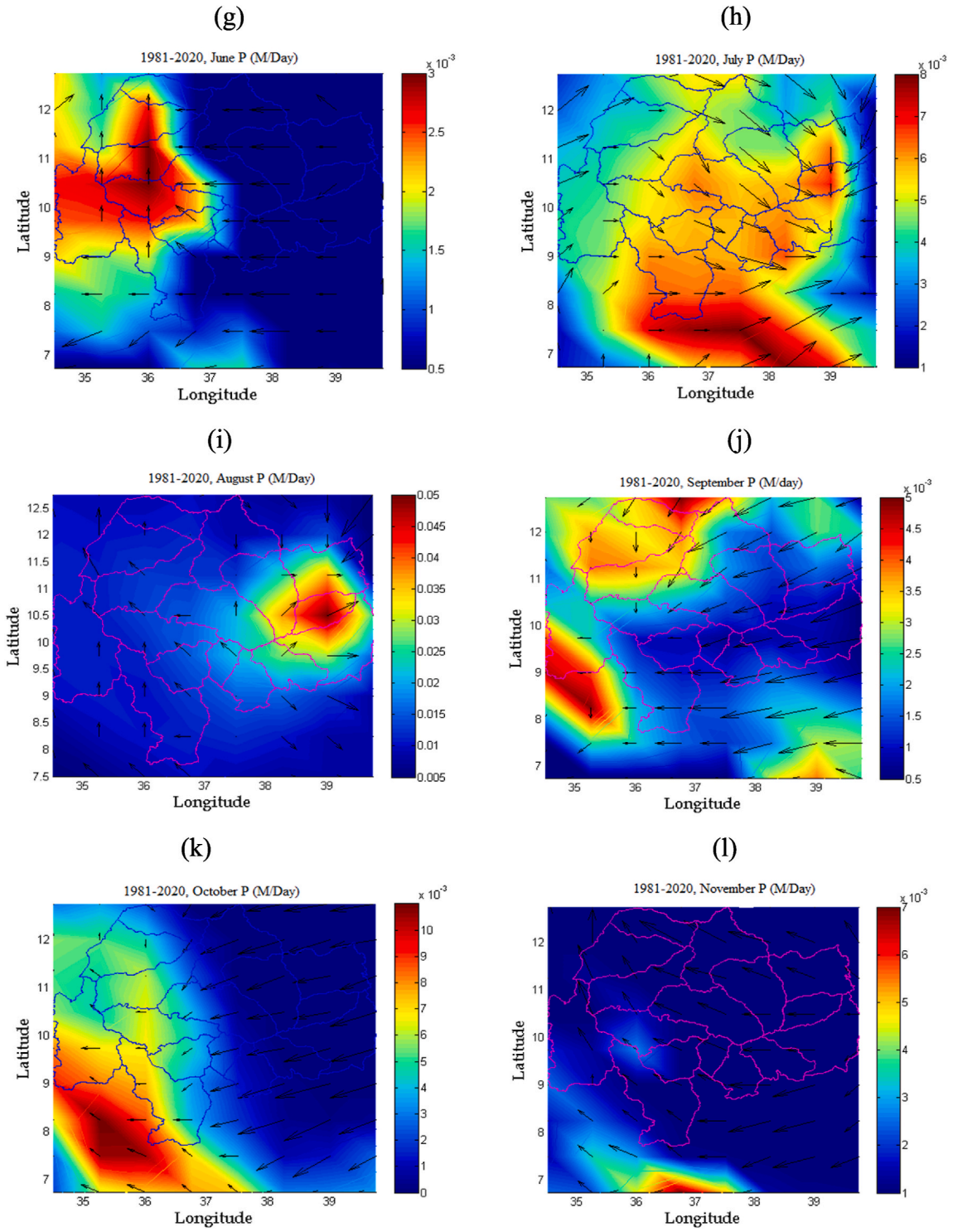


**Fig. 3.** (*continued*).

## 3. Results and discussion

The value of the improved model parameter found that b is 0.1000 and c is 0.2000 which can be calculated by applying the least square method from (Eq. (4)) after calculating yk from (Eq. (3)) which satisfied the model requirements. This paper considers precipitation and temperature prediction since the other parameters such as surface pressure, incident solar radiation, total evaporation, U

and V wind are used in the input of the model (Fig. 2).

The impact of atmospheric attributes on precipitation and temperature prediction is provided in Table 2. Indeed, the correlation (R) between precipitation with temperature, surface pressure, incident solar radiation, total evaporation, U and V wind are found −0.544, −0.208, −0.516, −0.687, 0.189, and 0.385 respectively. The main reason for the negative correlation between precipitation and evaporation is due to the direction difference of its dynamics (precipitation has a downward and evaporation upward direction). Because of the lack of seas and oceans over UBNB in Ethiopia, the R between precipitation and temperature is negative. Hence, there is a high temperature that may not get proportional to evaporation and no cloud formation which converted to precipitation due to the lack of enough moisture budgets in the atmosphere. Indeed, sometimes little moisture is available in the atmosphere from UBNB Rivers and lakes. However, this moisture is not rich in precipitation because advection wind moves the moisture to the neighboring countries such as Egypt and Sudan before reaching maximum thermodynamic points [35]. Similarly, the correlation between precipitation and surface pressure is negative; the reason is that the pressure gradient force of UBNB is high since it is a highland area. The high-pressure gradient forces diverge atmospheric moisture to the surroundings and not contributed to the precipitation in the vicinity.

Surface radiation has the same role as the temperature that affects precipitation. However, precipitation positively correlated to U and V winds. This is because U wind carried moisture from the Indian Ocean and contributed spring season precipitation in the eastern part of UBNB and V wind carried moisture from the Atlantic Ocean and contributed summer precipitation in the central and western parts of UBNB [35]. The study conducted by Litta et al. [39] in Kolkata west Bengal found nearly similar results to this finding using similar input parameters of the model. Climate prediction using a neural network model was conducted by Rajendra et al. [28] at Ongole and their findings strongly supported this paper's finding. Statistically significant R among temperature, precipitation, and evaporation are observed among the rest parameters with a statistical level of 0.05 as provided in Table 2. However, this paper considers precipitation and temperature prediction outputs since the other parameters are used in the input of the model (Fig. 2). By considering atmospheric attributes, spatial and temporal variability of precipitation and the diving parameters of the wind are provided in Fig. 3. This is help to the starting time for precipitation and temperature prediction.

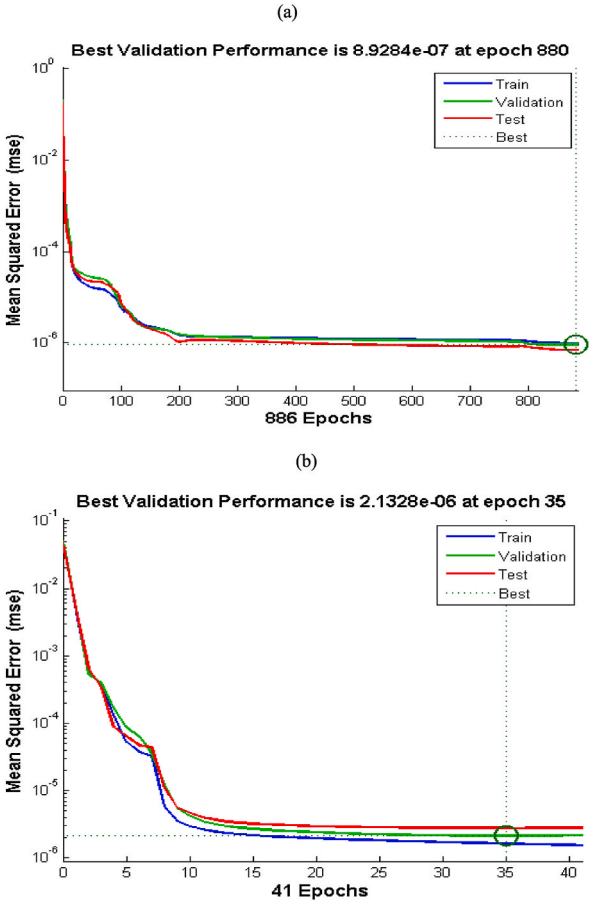


**Fig. 4.** The performance iteration of 886 is ending at epoch 880 which is represented on the top panel (a) and from 41 iterations is found best fitting at epoch 35 which indicated the bottom panel (b) for the test, train, and validation over UBNB.

### 3.1. Space and time variability of precipitation over UBNB

The daily average monthly precipitation variability due to moisture-carrying winds is provided in Fig. 3(a)–3(l). Since the atmospheric moisture budget is one of the core parameters of climate (precipitation and temperature) prediction [35]. Furthermore, the U and V wind is very important to show the dynamics of the atmospheric moisture for nowcasting and forecasting the weather as well as the climate over the UBNB as shown in Figs. 3–5. The spatiotemporal trend value of the atmospheric moisture is provided in Fig. 3 and is used as the indicator of the ANN model precipitation and temperature prediction.

The sources of little precipitation during December and January for UBNB are the Red Sea, the Arabian Sea, and local moisture as shown in Fig. 3 (a) and Fig. 3 (b). Similarly, precipitation is coming from the Arabian Sea, very little from the Indian Ocean and local moisture during February and contributed to the precipitation over the study area as we can see the wind direction and divergence in

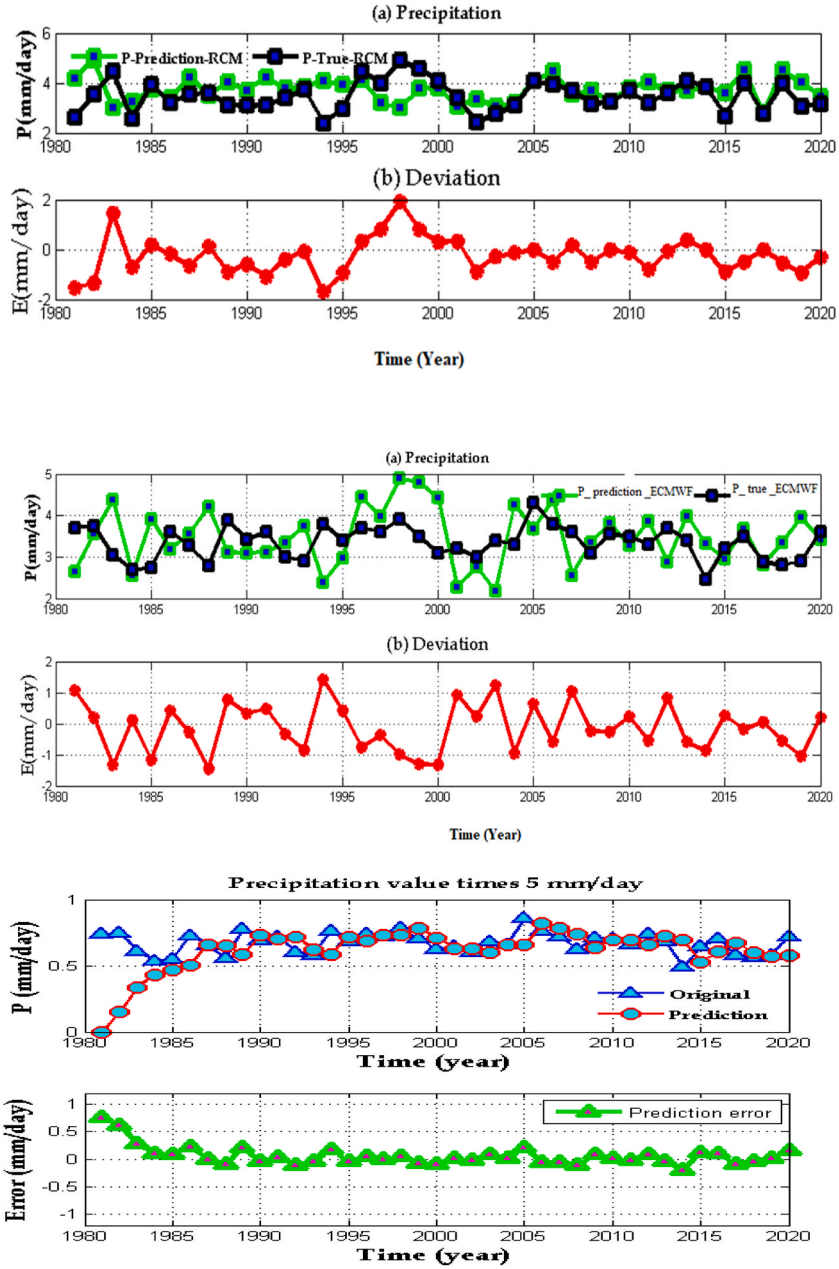


**Fig. 5.** Annual precipitation data prediction performances and errors from RCM data are provided in the top panels (a) and (b), from the ECMWF model middle panels (a) and (b), and ANN in the bottom panel. The ANN model precipitation data is normalized and the legend must multiply by 5 mm/day to get the true value but not the error terms.

Fig. 3 panel (c). During March, the sources of little precipitation is coming from Indian Ocean moisture and fronted with local moisture that contributed to the southern parts of UBNB; while during April, there is a lack of precipitation in the study area except for the southern end parts as shown in Fig. 3 at panels (d) and (e) respectively. This is because during April the dominant winds are northerly and northeast which is very dry due to the lack of Oceans in the northern hemisphere [42]. During May and June (see Fig. 3 at panels (f) and (g)), the sources of precipitation are the Indian Ocean, whereas in July (see Fig. 3 at panel (h)) it comes from the Atlantic Ocean and it confirmed by different literatures such as reference [35]. But during August, the sources of precipitation are the convergence between local moisture and the Atlantic Ocean moisture (see the wind vectors in Fig. 3 (i)). During September and October, the sources of precipitation are the Indian Ocean and the Red Sea moisture carried by strong trend winds, while during November the sources of precipitation are southern and eastern winds as shown in Fig. 3 at panels of (j), (k), and (l). Estimation of wind vector from moisture budget is quite useful for accurate prediction of the local climate using different models. This finding is supported by Refs. [35,43], who studied the climatological variation of the global and local dynamics of atmospheric moisture over UBNB and slightly disagree with the study conducted by Ref. [42] on Ethiopia.

### 3.2. *Characterizing the training, validation, and test model performance based on error matrices*

The entire curve (training, validation, and test) does not have the major problems shown in Fig. 4 at panels (a) and (b).

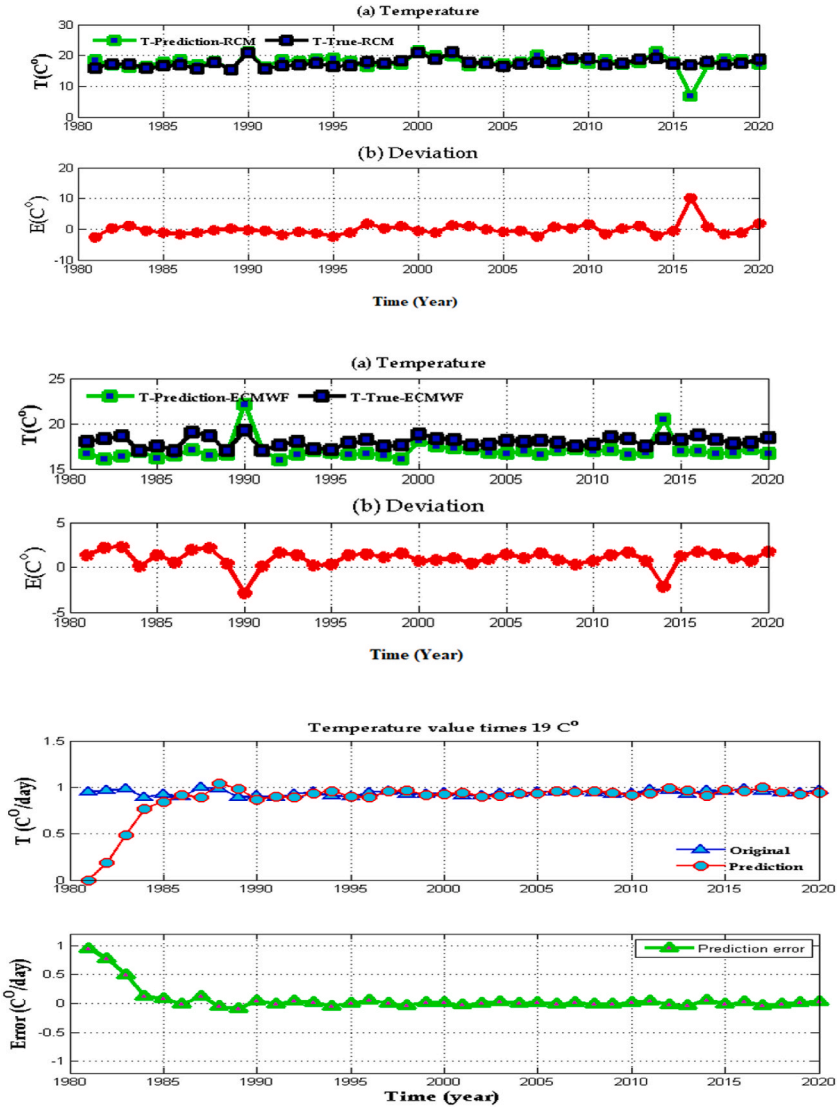


**Fig. 6.** Annual temperature prediction and error analysis from RCM data has been provided in the top panels (a) and (b); from the ECMWF model at the middle panels of (a) and (b), and ANN in the bottom panel. The ANN model temperature legend should be multiplied by 19 °C to get the true value but not in error terms since the prediction iteration was normalized.

Furthermore, the test curve is not increased notably before the validation curve increases. This is strongly supported by Beale et al. [44], whereas disproved the assumption of which was conducted by Kourosh et al. [45]. In this paper, the best network structure is found at epoch 886 and the performance may not necessarily be improved even if an iteration is reached 1000. It is observed from Fig. 4 panel (b), the performance of training, testing, and validation errors were minimized because of the improvement of the ANN model by IRF. When an epoch is found at 35, the performance needs further improvement in the network and it seems to have an outlier as shown in panel (a) of Fig. 4. Precipitation prediction using ANN models for time-series data is conducted and analyzed by Neelam et al. [26] and they found good results at epoch 12. Furthermore, they tried to estimate the training, validation, and testing value of the regression model and they found R-values are 0.9350, 0.9460, and 0.9480 respectively. However, in this paper, R was found to be 0.9980 after improving the ANN model by IRF. The curve model is quite useful to check the performance of the improved ANN for training, validation, and test model as shown in Fig. 4 at panels of (a) and (b).

### 3.3. The comparisons of ANN model performance with RCM, and ECMWF before applying IRF

The temporal comparison of precipitation and temperature history data with prediction data from RCM, ECMWF, and ANN models is provided in Figs. 5 and 6. The prediction of precipitation and the true observation data from RCM is indicated by different colors as shown in Fig. 5 at panel (a). Prediction performance of precipitation data from RCM using error matrices is provided in Fig. 5 (b). The BR, R, and RMSE between prediction and the actual data are found 0.9450, 0.4080, and 2.9700 respectively. Furthermore, the performance of temperature data from RCM is found at 1.0170, 0.4350, and 2.6600 respectively as we can see from Fig. 6 at panels (a) and (b). Similarly, the prediction performance of precipitation data from ECMWF using error metrics is provided in the middle Fig. 5 (a) and (b). The BR, R, and RMSE between prediction and true data are found 1.0030, 0.3530, and 3.1700 respectively. Similarly, the performance of temperature data from ECMWF; the BR, R, and RMSE are found at 1.0583, 0.4090, and 3.2300 respectively as shown from middle Fig. 6 (a) and (b); while the prediction performance of precipitation from the ANN model is provided in the two bottom panels of Fig. 5. The BR, R, and RMSE between prediction and true data are found at 1.0010, 0.7610, and 0.6200 respectively. However, a significant difference is observed after the improvement of the ANN model by IRF as shown in Table 3.

The range of RCM mean relative errors between the prediction of temperature data and the true value varied from −5 to 10 °C with an average of 0.0300 °C (see Fig. 6 at panels (b) and (c)); while from ECMWF varied from −5 to 5 °C with an average of 0.0100 °C (see middle panel b and c of Fig. 6). Furthermore, from the ANN model varied from 0 to 1 °C with an average of 0.0002 °C as shown in the bottom panel of Fig. 6; whereas from the ECMWF model based on BR, R, and RMSE are found at 1.0583, 0.4090, and 3.2300 respectively. Similarly, from the RCM model were found at 1.0168, 0.4350, and 2.6600 respectively; while from the ANN model, BR, R, and RMSE are found at 1.0004, 0.6630, and 0.7300 respectively as shown in Table 3. Even though, before the improvement of the ANN model by IRF, its performance is much better than ECMWF and RCM model performances for climate prediction.

### 3.4. The spatiotemporal prediction of precipitation and temperature after improvement of the ANN model by IRF

The trend analysis of ANN model precipitation and temperature prediction from 2020 to 2050 after applying IRF is provided in Fig. 7. The negative trend value of precipitation is expected from 2022 to 2023, 2030–2034, 2044–2049, and the maximum value of precipitation will be expected in the years from 2024 to 2029, 2035–2037. Similarly, a decrement trend of temperature over the study area from 2021 to 2025 excluding 2023 and 2028–2034 is expected, whereas from 2035 to 2050 excluding 2039 and 2043 the increment in temperature will be expected as shown in Fig. 7. Temperature trend analysis indicated that the occurrence of extreme events′ frequency is opposite to precipitation as shown in Fig. 7. The study was conducted by Refs. [46,47] stated that in 2015 severe drought due to the occurrence of El-Nino was observed in Ethiopia. Similarly, in 2002 significant drought happened in Ethiopia [48]. Therefore, this finding strongly supported the above pieces of evidence as shown in Figs. 7 and 8.

After the prediction of precipitation and temperature time-series data, the spatial distribution has been estimated by applying CDO software from 2020 to 2050. The annual average value of precipitation from 1981 to 2020 is found 1050 mm (see Fig. 8 (a)). The spatial distribution prediction of precipitation was the same but a little bit different in its magnitude. Indeed, the annual average value

**Table 3**
Estimation of error metrics between history and prediction precipitation and temperature data from 1981 to 2020 based on the European Center of Medium Range Weather Forecast (ECMWF), Regional Climate Model (RCM), and Artificial Neural Network (ANN) model before application of Impulse Response Function (IRF) and precipitation prediction after improvement by IRF (P_ANN_IRF) and temperature prediction after improvement by IRF (T_ANN_IRF).

| Parameter | BR | R | RMSE |
|---|---|---|---|
| P_ECMWF | 1.0032 | 0.353 | 3.67 |
| T_ECMWF | 1.0583 | 0.409 | 3.23 |
| P_RCM | 0.9453 | 0.408 | 2.97 |
| T_RCM | 1.0168 | 0.435 | 2.66 |
| P_ANN | 1.0012 | 0.761 | 0.62 |
| T_ANN | 1.0004 | 0.663 | 0.73 |
| P_ANN_IRF | 0.9978 | 0.863 | 0.37 |
| T_ANN_IRF | 1.0002 | 0.742 | 0.89 |

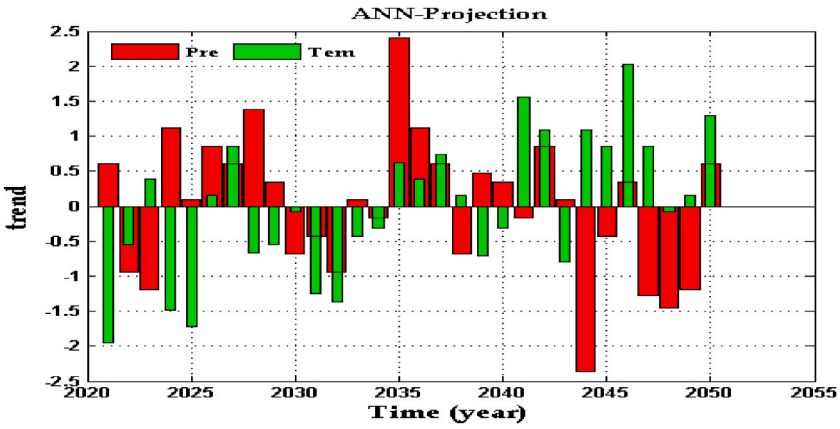


**Fig. 7.** Precipitation and temperature from the ANN model predicted value and its trend analysis. Prediction from the ANN model bottom left panel.

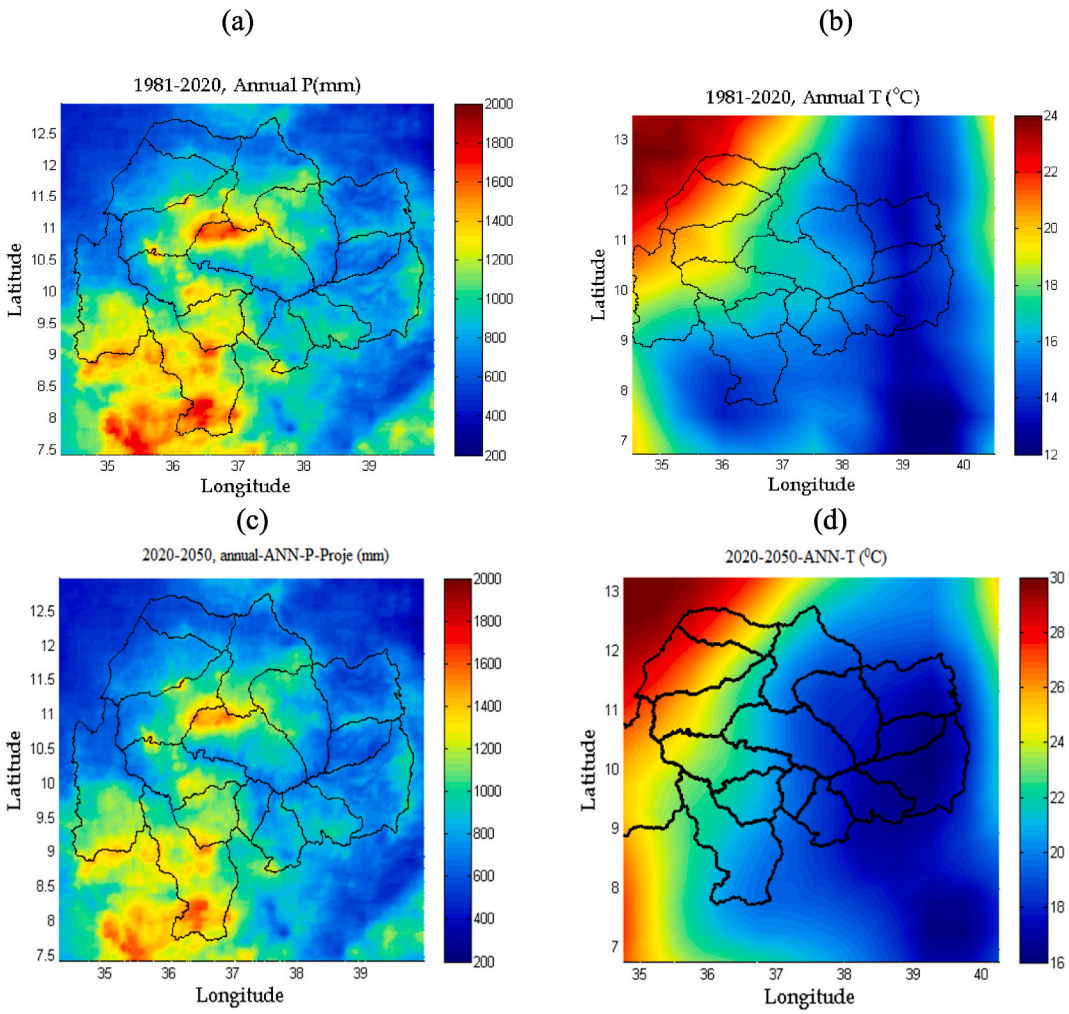


**Fig. 8.** Annual history precipitation data from ECMWF model represented at top left panel (a), history mean annual daily temperature data from ECMWF top right panel (b), precipitation ANN model prediction data bottom left panel (c), and temperature prediction from ANN model bottom left panel (d).

of precipitation predictions (2020-250) was found 997 mm (see Fig. 8 (c)). Whereas the prediction of temperature data from ECMWF model represented in Fig. 8 (b) and from ANN model in Fig. 8 (d). The spatial prediction of precipitation is indicated that in the next 30 years in the south, southwest, and central parts of the UBNB will be decreased as shown in Fig. 8.

After improving the ANN model by IRF, precipitation and temperature prediction from 2020 to 2051 are provided in Fig. 9. In the period of 2032, 2042, and 2049, the maximum precipitation will be expected, while the minimum value will occur during 2035, 2045, and 2050. Similarly, the maximum temperature occurrences years will be found in 2033 and 2043, whereas minimum years will be found in 2036 and 2044. The precipitation axis value plus 2.4 mm gives the true value of the data to show the error on the same precipitation axis since the data is normalized between 0 and 1 but not added 2.4 mm on the error axis (Fig. 9 (a)). The training is made from 1981 to 2011 from the input data to test up to 2020, then to predict from 2021 to 2051 by considering the sampling markers as provided in Fig. 9 (a). The range of actual precipitation and prediction data varied from 2.600 to 4.000 mm. The network is trained and tests the validation from 1981 to 2011 and sampled to 2051. Hence, the prediction is done by gathering information from the training and forecast up to 2051. The annual average value of the error is found 0.0012 mm. Precipitation prediction was conducted with a learning rate of 0.1000 by Litta et al. [39] and they found similar results to these findings before the improvement of the ANN model by IRF, whereas this finding is more accurate after improvement by IRF as shown in Table 3. Similarly, the ANN model in the prediction of meteorological parameters during pre-monsoon thunderstorms was studied by Litta et al. [39] at Kolkata in West Bengal; R and RMSE of temperature prediction were found 0.9500 and 1.8900 respectively. In this paper, the temperature prediction before IRF application R is found 0.6600 and RMSE is 0.7300, while after applying the application of IRF, R is 0.7400 and RMSE is 0.8900. In the case of RMSE the model improvement is not that significant but in the case of R shows good improvement. The prediction of the climate parameters

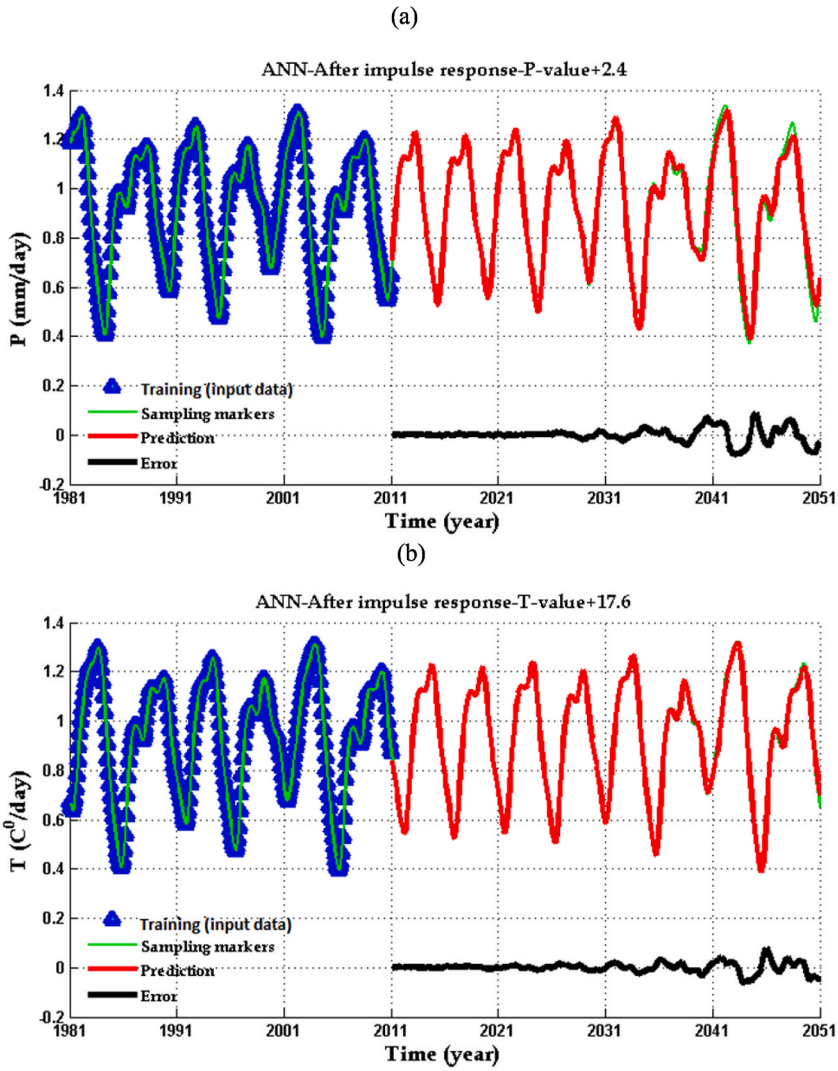


**Fig. 9.** Precipitation panel (a) and Temperature panel (b) prediction, training, sampling markers, and error analysis after improved ANN model by IRF. After improving the ANN model by IRF, the color is represented as Blue for input (training) data, Red for forecasting, Green for orientation indicator sampling markers, and Black is the error deviation between history and prediction data.

showed good performance which was conducted by Litta et al. [39] based on R but it is poor in the case of RMSE to compare with this finding. The deviation may be raised to the study area and time differences.

After the improvement of the ANN model by IRF, the temperature prediction from 2020 to 2051 is provided in the bottom pane of Fig. 9 (b). The temperature axis value plus 17.6000 °C gives the true value of the data because of the arrangement of the temperature axis like precipitation. A range of temperature history and prediction data varied from 17.7000 to 19.0000 °C. Indeed, the mean value of the error is found −0.0120 °C. Hence, temperature prediction is less accurate than precipitation. The accuracy of the ANN model before improvement by IRF is effective for up to 20 years (up to 2041). However, its accuracy is decreased for long-year prediction since the model is difficult to memorize the training data for a long period; while it is effective for up to 30 years when the ANN model is improved by IRF as shown in Fig. 9. Precipitation and temperature prediction using the statistical downscaling model was studied by Temesgen et al. [49] at UBNB, Ethiopia and they found similar results to RCM and ECMWF model precipitation prediction with this paper results. Similarly, the range of annual average daily history temperature data from 1981 to 2020 varied from 12 to 24 °C with an average value of 19 °C. Consequently, temperature prediction shows a slight spatial distribution variation and a significant magnitude difference is observed between the history and the prediction data. Hence, the range of temperature prediction data from 2020 to 2050 value varied from 16 to 30 °C with an average value of 24 °C. Therefore, in the next 30 years, the temperature will be increased as shown top and bottom-right panels of Fig. 8. Such kind of spatial temperature and precipitation distribution prediction was done by Ref. [46], and their prediction was very close to this finding.

As observed different climate predictions using ANN model literature, for instance, Akash and Smcs [50] are effective for short-term predictions but not long periods. However, in this paper, the prediction error is acceptable to predict the climate for 30 years as shown in Fig. 9. As illustrated in Fig. 9, the prediction error is almost zero up to near 2041. Indeed, after 2041 to 2051 the prediction error is a float from −0.2000 to 0.2000 which is still an acceptable error and the prediction model is working well. The maximum temperature prediction value is observed in 1991, 2002, and 2014 as shown in the bottom panel of Fig. 9 (b). This year's maximum temperature and minimum precipitation are found due to the occurrence of space weather over UBNB which was studied by Megbar and Shimelis [51]. Therefore, the prediction results are trustful by providing promising shreds of evidence.

The statistical indicators are used to assess the performance ANN model before and after intervention with IRF models and the results are compared to different literature [52–54] that considers large-scale dynamics (El Nino and La Nina events) for climate change prediction. Owing to this, the improved ANN model produced reasonably accurate results and it is showing good agreement with past studies. Indeed, Gebrekidan et al. [55] compared the prediction of precipitation and temperature data to the historical data using statistical techniques and they found that R is 0.5270 and 0.4110 over UBNB. In this finding, the prediction of precipitation and temperature from the RCM model data R is found at 0.4070 and 0.4350 respectively which is consistent with [55]; while ANN prediction of this finding is more accurate than the prediction which was conducted by Ref. [55].

Similarly, precipitation and temperature prediction by using GCM and ANN models was done by Ref. [23] in Saudi Arabia. They found the R between history and predicted data varied from 0.4200 to 0.6300 for the GCM model and from 0.5000 to 0.7000 for the ANN model respectively. In this finding, the RCM model is nearly similar to GCM and ANN with itself. However, after the improvement of the ANN model by IRF, the prediction of precipitation and temperature is more accurate than the findings of [23].

Precipitation and potential evaporation were forecasted by Getachew and Yuei [11] using the ANN model which is very good to predict time-series signatures with high coefficients of determination and low RMSE values were 0.7530, 0.8070, and 1.1260 for the two-layer ANN, one-layer ANN, and linear models, respectively. They conclude that the ANN models were far better to predict new data than the linear model. However, the ANN model after being improved by IRF is the most accurate since an average value of RMSE is found at 0.3700. Even though, in this finding ANN model before the applied IRF is slightly better than [11] because the RMSE is found 0.6200 as shown in Table 3.

The research finding of Asmaa et al. [43] indicated the prediction of precipitation over the Blue Nile, Ethiopia. They found the R-value of 0.8170 by comparing the prediction and the true data from 1985 to 2015. In this paper, to compare the prediction and true value of precipitation data from 1981 to 2020 over UBNB by applying the ANN model before improvement; R is found 0.7610. In this paper, the prediction skill of the ANN model is weaker than Asmaa et al. (2019) prediction, while after the improvement of the ANN model by IRF, R-value is enhanced from 0.7610 to 0.8630. After the improvement of the ANN model by IRF is effective to predict the climate elements over variable topography feature area with comparison to Refs. [43,50] as shown in Fig. 9. After the improvement of the ANN model by IRF, BR from 1.0012 reduced to 0.9978, R from 0.7610 increased to 0.8630, and RMSE from 0.6200 reduced to 0.3700 for precipitation prediction. Whereas for temperature prediction, BR from 1.0004 reduced to 1.0002, R from 0.6630 to 0.7420, and RMSE from 0.7300 to 0.8900. After the improvement of the ANN model by IRF, the prediction of precipitation is the best trustful based on the three error matrices (BR, R, and RMSE). Similarly, temperature prediction shows very good improvement based on BR and R but not good on RMSE see Table 3. Therefore, in this paper, the model improvement is well trustful for climate prediction for up to 30 years over UBNB in Ethiopia.

## 4. Conclusions and recommendations

ANN model is applied for precipitation and temperature prediction over the UBNB. Owing to this, several annual climate indices and the areal average precipitation and temperature of the UBNB are used as predictors and a predictor of the ANN model, respectively. The optimal hidden neuron number of the ANN model with 7 input variables is selected based on error matrices including the *P*-value. A preliminary ANN model showed satisfactory prediction performance with BR, R, and RMSE than RCM and ECMWF for the training, validation, and testing model. The results also indicated that the quantification of the contribution of the variable's relative importance can improve the accuracy of climate forecasts by adding some input variables for precipitation and temperature-controlling factors.

The prediction results revealed that the improved ANN model by IRF is more successful in reducing errors than before the improved ANN model by IRF of the UBNB.

After the improvement of the ANN model by IRF, the precipitation prediction error is reduced by 10.2 %; whereas the temperature prediction error is reduced by 7.9 % over UBNB. Hence, based on the improved ANN model results, the temperature has increased over the past 40 years, and it is expected to continue for the coming 3 decades (30 years). Contrary, precipitation over the past 40 years has decreased and a slight increment will occur in the next 8 years (2021, 2024–2029) and it will decrease for the coming 5 years (2030–2034), whereas from 2035 to 2040 will be increased, and decrease from 2041 to 2050. Consequently, in the future, at the central, southern, and southwest parts of the UBNB, the lack of precipitation will be more occurred than in the rest parts. Whereas in the western part of the UBNB, the enhancement of temperature will be expected. Generally, the improved ANN model is quite useful for the spatiotemporal climate prediction over variable topography feature areas like UBNB. Hence, clear awareness should be created for the local community by providing the extreme climate occurrence frequency which helps them to fix crop selection for the next 30 years of agriculture production.

## Data availability statement

The data that has been used is confidential and it will be made available on request.

## Additional information

No additional information is available for this paper.

## CRediT authorship contribution statement

**Megbar Wondie:** Conceptualization, Formal analysis, Methodology, Software, Validation, Visualization. **Titike Kassa:** Data curation. **Demeke Fisseha:** Writing – original draft.

## Declaration of competing interest

The authors declare that there is no conflict of interest regarding the publication of this paper.

## Acknowledgments

The authors are very pleased to the Ethiopian Space Science and Technology Institute for its constant financial support throughout the time of the research. The authors also acknowledge the College of Natural and Computational Science, Debre Markos University, Ethiopia for its material and car support for the field visit. We would also like to express our appreciation to the Ethiopian Meteorology Agency offices for their well-coming approach and support to high-resolution climate data. We would like to thank you colleagues for surrounding us and for your substantial involvement in the research in one or another way.

## References

[1] J. Sillmann, et al., Understanding, Modeling and Predicting Weather and Climate Extremes: Challenges and Opportunities, Weather and Climate Extremes, 2017, https://doi.org/10.1016/j.wace.2017.10.003.
[2] J. Gregory, et al., Developing seasonal rainfall scenarios for food security early warning, Theor. Appl. Climatol. 114 (2013) 291–302.
[3] S. Abeer, G. Mona, Ibrahim, E.M. Wael, F. Manabu, E. Amr, D. Waled D, Statistical assessment of rainfall characteristics in upper Blue Nile Basin over the period from 1953 to 2014, Water 11 (2019) 468, https://doi.org/10.3390/w11030468.
[4] P. Nastos, K. Moustris, I. Larissi, A. Paliatsos, Rain intensity forecast using artificial neural networks in Athens, Greece, Geophys. Res. Abstr. 12 (2010).
[5] A.C. Subhajini, Application of neural networks in weather forecasting, Inter. J Weather Climate Change Conser. Res. 4 (1) (2018) 8–18.
[6] R. Vincent, L. Tatenda, GeteZeleke, T.S. Alemtsehay, K.N. Tibebu, H. Hans H, Effects of climate change on water resources in the upper Blue Nile Basin of Ethiopia, Heliyon 4 (2018), e00771.
[7] E. Abdelrazek, Z. Hongwei, W. Bingfang, A. Ayele, Fenta, N. Mohsen, D. Robert, Soil Erosion Assessment in the Blue Nile Basin Driven by a Novel RUSLE-GEE Framework, Science of The Total Environment, 2021, https://doi.org/10.1016/j.scitotenv.2021.148466.
[8] M. Belayneh, T. Yirgu, D. Tsegaye, Effects of soil and water conservation practices on soil physicochemical properties in Gumara watershed, Upper Blue Nile Basin, Ethiopia, Ecol Process 8 (2019) 36, https://doi.org/10.1186/s13717-019-0188-2.
[9] WFP Ethiopia Country Brief, 2020.
[10] M.A. Mariam, J.F. Anjuli, B.M.L. Dennis, A.B. Elfatih, Estimation of evaporation over the upper Blue Nile basin by combining observations from satellites and river flow gauges, Am. Geophys. Union. Res 52 (2016), https://doi.org/10.1002/2015WR017251.
[11] M.M. Getachew, A.L. Yuei, Application of artificial neural networks in forecasting a Standardized precipitation Evapotranspiration Index for the upper Blue Nile Basin, Water 12 (3) (2020) 643, https://doi.org/10.3390/w12030643.
[12] A. Kumar, M.P. Singh, G. Saswata, A. Abhishek, Weather forecasting model using artificial neural network, Procedia Technol. 4 (2012) 311–318.
[13] G.I. Diro, E. Black, D.I.F. Grimes, Seasonal forecasting of Ethiopian spring rains, Meteorol. Appl. 15 (2008) 73–83.
[14] R.N. Deepak, M. Amitav, M. Pranati, A Survey on rainfall prediction using artificial neural network, Inter. J. Comp. Appl. 72 (16) (2013), 0975 – 8887.
[15] R.D. Rohit, On the rainfall time series prediction, using multilayer Perceptron artificial neural network, IJETAE 2 (2012) 1.
[16] F.F. Hattermann, V. Krysanova, S. Gosling, R. Dankers, P. Daggupati, C.H. Donnelly, M. Flörke, S. Huang, Yu Motovilov, S.S. Buda, et al., Cross-scale inter-comparison of climate change impacts simulated by regional and global hydrological models in eleven large river basins, Clim. Change 141 (2017) 561–576.
[17] Y. Peng, X. Zhao, D. Wu, B. Tang, P. Xu, X. Du, H. Wang, Spatiotemporal variability in extreme precipitation in China from observations and projections, Water 10 (2018) 1089.

[18] D.F. Mekonnen, M. Disse, Analyzing the future climate change of the Upper Blue Nile River basin using statistical downscaling techniques, Hydr. Earth Syst. Scie. 22 (2018) 2391–2408.
[19] S.L. Sorland, C. Schar, D. Luthi, E. Kjellstrom, Bias patterns and climate change signal in GCM, RCM model chains, Environ. Res. Lett. 13 (2018), 74017.
[20] E. Bucchignani, P. Mercogliano, H.J. Panitz, M. Montesarchio, Climate change projections for the Middle East-North Africa domain with COSMO-CLM at different spatial resolutions, Adv. Clim. Change Res. 9 (2018) 66–80.
[21] V. Krysanova, T. Vetter, S. Eisner, S. Huang, I. Pechlivanidis, M. Strauch, A. Gelfan, R. Kumar, A. Aich, B. Arheimer, et al., Inter-comparison of regional-scale hydrological models and mate change impacts projected for 12 large river basins worldwide a synthesis, Environ. Res. Lett. 12 (2017).
[22] P. Zelazowski, C. Huntingford, L.M. Mercado, N. Schaller, Climate pattern-scaling set for an ensemble of 22 GCM-adding uncertainties to the IMOGEN version 2.0 impact system, Geosci. Model Dev. (GMD) 11 (2018) 541–560.
[23] A. Khalid, R. Abdul, H. Ghumman, M.G. Yousry, M.D. Shafiquzzaman, Future predictions of rainfall and temperature using GCM and ANN for arid regions: a case study for the Qassim region, Saudi Arabia, Water 10 (2018) 1260, https://doi.org/10.3390/w10091260.
[24] P. Singh, B. Borah, Indian Summer Monsoon Rainfall Prediction Using Artificial Neural Network, Stochastic Environmental Research and Risk Assessment, 2013, pp. 1436–3240.
[25] C. Funk, P. Peterson, M. Landsfeld, D. Pedreros, J. Verdin, S. Shukla, G. Husak, J. Rowland, L. Harrison, A. Hoell, J. Michaelsen, The climate hazards infrared precipitation with stations a new environmental record for monitoring extremes, Sci. Data 2 (2015) 1–21, https://doi.org/10.1038/sdata.2015.66.
[26] M. Neelam, K. Hemant, S. Sanjiv, Upadhyay, Development and analysis of artificial neural network models for rainfall prediction by using time-series data, I, J. Intel. Sys. Appl. 1 (2018) 16–23.
[27] Haviluddin Mislan, Sumaryono H. Sigit, A. Marlon, Rainfall monthly prediction based on artificial neural network:A case study in Tenggarong station, East Kalimantan - Indonesia, Procedia Comp. Sci. 59 (2015) 142–151.
[28] K.V.N. Rajendra, A. Subbarao, B. Rahul, Use of ANN Models in the Prediction of Meteorological Data, Modeling Earth Systems and Environment, 2019, https://doi.org/10.1007/s40808-019-00590-2.
[29] D. Katherine, M. Benjamin, A.F. Rosie, M. David M, A machine learning approach to emulation and biophysical parameter estimation with the Community Land Model, version 5, Adv. Stat. Clim. Meteorol. Oceanogr. 6 (2020) 223–244, https://doi.org/10.5194/ascmo-6-223-2020.
[30] P.D. Dueben, P. Bauer, Challenges and design choices for global weather and climate models based on machine learning, Geosci. Model Dev. (GMD) 11 (2018) 3999–4009, https://doi.org/10.5194/gmd-11-3999.
[31] S. Scher, Toward data-driven weather and climate forecasting: Approximating a Simple general circulation model with deep learning, Geophys. Res. Lett. 45 (2018) 12616–12622, https://doi.org/10.1029/2018GL080704.
[32] S. Sebastian, M. Gabriele, Weather and climate forecasting with neural networks: using general circulation models (GCMs) with different complexity as a study ground, Geosci. Model Dev. (GMD) 12 (2019) 2797–2809, https://doi.org/10.5194/gmd-12-2797-2019.
[33] S. Amir, C. Fuat, K. Farzad K, A method for forecasting weather conditions by using artificial neural network algorithm, APRIL, VOLUME, ICTACT J. Soft Comp. 8 (2018) 2229–6956, https://doi.org/10.21917/ijsc.2018.0237.
[34] W. Abera, F. Giuseppe, B. Luca, R. Riccardo, Water budget modeling of the upper Blue Nile basin using the JGrass-NewAge model system and satellite data, Hydrol. Earth Syst. Sci. 21 (2017) 3145–3165, https://doi.org/10.5194/hess-21-3145-2017.
[35] W.B. Megbar, U. Jaya Prakasha, T.K. Samuel, Estimating the role of upper Blue Nile basin moisture budget and recycling ratio in spatiotemporal precipitation distributions, J. Atmos. Sol. Terr. Phys. 193 (2019), 105064, https://doi.org/10.1016/j.jastp.2019.105064.
[36] D. Conway, The climate and hydrology of the upper Blue nile, Ethiopia, Geogr. J. 166 (2000) 49–62.
[37] W.B. Megbar, U. Jaya Prakasha, T.K. Samuel, Estimation of rainfall intensity from first observation weather radar reflectivity data over upper Blue Nile Basin, Ethiopia, Trans. Sci. Technol 5 (No. 4) (2018) 223–232.
[38] W. Megbar, Modeling cloud seeding technology for rain enhancement over the arid and semiarid areas of Ethiopia, Elsevier, ScienceDirect, Heliyon 9 (2023), e14974, https://doi.org/10.1016/j.heliyon.2023.e14974.
[39] A.J. Litta, M.L. Sumam, U.C. Mohanty, Artificial neural network model in prediction of meteorological parameters during Premonsoon thunderstorms, Hindawi Publ. Corp. Inter. J. Atmospheric Sci. (2013), 525383, https://doi.org/10.1155/2013/525383, 14 pages.
[40] W. Jianxin, G. Lamda, Introduction to Convolutional Neural Networks National Key Lab for Novel Software, Technology Nanjing University, China, 2017.
[41] L. Jeongwoo, K. Chul-Gyum, E.L. Jeong, W.K. Nam, K. Hyeonjun, Application of artificial neural networks to rainfall forecasting in the Geum river basin, Korea, Water 10 (2018) 1448, https://doi.org/10.3390/w10101448.
[42] D. Korecha, A.G. Barnston, Predictability of June-September rainfall in Ethiopia, Mon. Weather Rev. 135 (2) (2007) 628–650.
[43] A. Asmaa, A. Ayele, Fenta, Y. Hiroshi, S. Katsuyuki, K. Takayuki, Prediction of summer rainfall over the source region of the Blue Nile by using teleconnections based on sea surface temperatures, Theor. Appl. Climatol. (2019), https://doi.org/10.1007/s00704-019-02796-x.
[44] M.H. Beale, M.T. Hagan, H.B. Demuth, Neural Network Toolbox User's Guide, The MathWorks, Inc, 2017.
[45] A. Kourosh, B. Chris, Z. Xingxing, Development of a predictive control model for a heat pump system based on artificial neural networks (ANN) approach, in: Master Level Thesis European Solar Engineering School No, 2019, p. 259.
[46] A. Juliana, and D. Jos´e, Neural Network Models for Climate Forecasting based on Reanalysis Data, X CongressoBrasileiro de Intelig^enciaComputacional (CBIC'2011), 8 a 11 de Novembro..
[47] G. Kelem, A. Derbew, The Frequency of El-Nino and Ethiopian Drought, ANM, 2017. https://www.researchgate.net/publication/317888587.
[48] W. Megbar, T. Tadesse, Assessment of drought in Ethiopia by using self-calibrated palmer drought severity index, (ScPDSI), I.J.E.M.S. 7 (2) (2016) 108–117. ISSN 2229-600X.
[49] G. Temesgen, T. Taffa, A. Mekuria, W. Abeyou, Worqlul, Modeling the hydrological impacts of land use/land cover changes in the Andassa watershed, Blue Nile Basin, Ethiopia, Sci. Total Environ. (2018) 1394–1408, https://doi.org/10.1016/j.scitotenv.2017.11.191, 619–620.
[50] D. Akash, Smcs-cest, Artificial neural network models for rainfall prediction in Pondicherry, 0975 888, Inter. J. Comp. Appl 120 (3) (2015).
[51] W.B. Megbar, T. Shimelis, Investigating the impact of space weather on agriculture products over the Chokie mountain basin in Ethiopia, ActaGeophysica 69 (2021), https://doi.org/10.1007/s11600-021-00610-9.
[52] A. El-Shafie, A. Noureldin, M.R. Taha, A. Hussain, Dynamic versus static neural network model for rainfall forecasting at Klang River Basin, Malaysia, Hydrol, Earth Syst. Sci. 8 (2011) 6489–6532.
[53] S.V.J. Soosani, K. Adeli, H. Fadaei, H. Naghavi, T.D. Pham, D.T. Bui, T. D, Improving accuracy estimation of forest aboveground biomass based on incorporation of ALOS-2 PALSAR-2 and sentinel-2A imagery and machine learning: a case study of the Hyrcanian forest area (Iran), Remote Sens 10 (2018) 172.
[54] J. Zhou, T. Peng, C. Zhang, N. Sun, Data pre-analysis and an ensemble of various artificial neural networks for monthly streamflow forecasting, Water 10 (2018) 628.
[55] W. Gebrekidan, T. Ermias, B. Amare, T.D. Yihun, Observed changes in extremes of daily rainfall and temperature in Jemma Sub-basin, upper Blue Nile Basin, Ethiopia, Theor. Appl. Climatol. 135 (2019) 839–854, https://doi.org/10.1007/s00704-018-2412-x.